ISSN 2176-5480

22nd International Congress of Mechanical Engineering (COBEM 2013)
November 3-7, 2013, Ribeirão Preto, SP, Brazil

THERMOGRAPHIC ANALYSIS OF ENERGY LOSS THROUGH THE ENGINE CYLINDER IN A COMPRESSION IGNITION ENGINE

Rafaela Bastos Campos
Anderson Flávio Bassi
Universidade Federal de São João del Rei , São João del Rei - MG - Brasil
rafaelacampos@live.com; anderson.bassi@yahoo.com.br

Felipe Cardoso Carvalho
Universidade Federal de São João del Rei , São João del Rei - MG - Brasil
carvalhofelipe.mec@gmail.com

Paulo Cezar Monteiro Lamim Filho
Universidade Federal de São João del Rei , São João del Rei - MG - Brasil
lamim@ufsj.edu.br

José Antônio da Silva
Universidade Federal de São João del Rei , São João del Rei - MG - Brasil
jant@ufsj.edu.br

Jorge Nei Brito
Universidade Federal de São João del Rei , São João del Rei - MG - Brasil
brito@ufsj.edu.br

Abstract. *Diesel engines are used in various economic sectors in the world, including transport and electricity generation. Such motors have remarkable durability and thermal efficiency among the basic configurations of internal combustions engines. It is considered as useful energy converted by the internal combustion engine that energy responsible for triggering its main axis. It is inside of an internal combustion engine cylinder that occurs complex phenomena of energy transformation, mainly by the combustion process. Heat transfer in engines affects their performance, efficiency and emissions. If large amount of heat is transferred to the walls of the combustion chamber, temperature and mean gas pressure decreases, reducing the work per cycle transferred to the cylinder. In this work we investigated the thermal exchanges that occur on the cylinder walls of a single cylinder diesel engine. Thermography was used for obtaining temperature measurements of the engine cylinder. As result a simple mathematical model for the process of heat loss around the cylinder of a single cylinder engine (Petter) will be presented.*

Keywords: *thermography, diesel engine, heat transfer*

1. INTRODUCTION

The energy losses in an internal combustion engine occurs by rejected heat in the exhaust gases, incomplete combustion, friction between moving parts, heat rejected by the cooling fluid, heat rejected by the lubricating fluid and heat rejected to the environment by the external surfaces of the engine. The activation energy of auxiliary systems (alternator, camshaft valves, fuel pump etc.) is derived from the work developed at the cylinders of the engine. Approximately, only 35% of the chemical energy that enters a internal combustion engine cycle are converted to useful energy in the crankshaft. Another 30% of fuel energy is rejected in the exhaust gases as chemical energy and enthalpy (PULKRABEK, 1997). Considering these levels, about one-third of fuel energy must be dissipated to the environment in some way, either by cooling and lubricating systems or through the external surfaces of the engine.

Heywood (1988) also states that about half the friction energy, the one consumed due to friction of all moving parts of the engine, is dissipated through the surface of pistons, piston rings and cylinders as thermal energy. The other part of this energy is dissipated by the surface of the other moving parts, by cooling and lubricant fluids.

Also according to Heywood (1988), heat transfer in the engine affects its performance, efficiency and emissions. If a large amount of heat is transferred to the combustion chamber walls, average pressure and temperature of gases decreases, reducing the work per cycle transferred to the cylinder.

The importance that has been given to the heat rejected by cylinder walls and consequently by the engine block, coolant fluids and lubricants, is so significant that several published papers deal with thermal efficiency gain analysis by insulation of these parts, mainly with ceramics materials.

ISSN 2176-5480

2. HEAT TRANSFER PROCESSES INSIDE THE CYLINDER

It is inside of an internal combustion engine cylinder that occurs complex phenomena of energy transformation, mainly by the combustion process. Alegre (1993) explains that during the processes that occurs in the engine cylinder, the working fluid undergoes large variations of temperature and pressure. These variations associated with the turbulent, transient and three-dimensional nature of flow, govern the behavior of heat exchange between the working fluid and cylinder walls, piston and cylinder head.

Considering the heat flow from the cylinder interior to the external environment, three modes of heat transfer occur: conduction, convection and radiation. Heat is transferred by convection and radiation from combustion gases to the cylinder wall. Then, by conduction, this energy reaches the outer surface and is rejected again by convection and radiation.

Besides the convective heat exchange, a considerable portion of energy is transferred by radiation in the cylinder interior coming from gases at high temperature and flame region to the cylinder walls. Radiation is also present at heat transfer from the engine external surfaces to the external environment, as well as convection due to air movement. Heywood (1988) explains that for a spark ignition engine the portion of heat transfer by radiation inside the cylinder can be neglected, the same does not apply to a compression ignition engine, once in this latter one the bright flame may appear at various points. There are also large radiation emission from solid particles formed mainly of carbon, which become incandescent. The radiation of these particles is approximately five times higher than the one of gases formed in the combustion process.

According to Jóvaj and Máslov (1973) the thermal balance of a compression ignition engine as given by in the Eq. 1 in which $\dot{Q}_0$ is overall rate of heat transfer to the engine by burning fuel at a given engine operating speed [W]; $\dot{Q}_e$ is heat transfer rate equivalent to the effective power measured by the dynamometer [W]; $\dot{Q}_{ref}$ is rate of heat rejected by the cooling fluid [W]; $\dot{Q}_g$ is rate of heat rejected in the exhaust gases [W]; $\dot{Q}_{cd}$ is rate of heat rejected in the exhaust gases corresponding to the portion of unburned fuel and incomplete combustion [W] and $\dot{Q}_{res}$ is heat transfer rate corresponding to other energy losses of the engine [W].

$$\dot{Q}_0 = \dot{Q}_e + \dot{Q}_{ref} + \dot{Q}_g + \dot{Q}_{cd} + \dot{Q}_{res} \quad (1)$$

In the balance proposed above $\dot{Q}_{res}$, which also comprises the heat rejected by the engine outer surface, normally is not detailed and its value is calculated by subtracting all other portions in relation to $\dot{Q}_0$. However, the overall rate of heat rejection to the environment by the outer surface of the engine cylinder can be calculated according to Eq. 2, in which heat transfer rate by radiation and convection portions are summed.

$$\dot{Q}_{Total} = \dot{Q}_{Conv} + \dot{Q}_{Rad} \quad (2)$$

Each plot can be obtained according to the Eq. 3 and Eq.4 in which $\dot{\mathbf{Q}}_{\mathbf{Total}}$ is total rate of heat rejection to the external environment [W]; $\dot{\mathbf{Q}}_{\mathbf{Conv}}$ is rate of heat rejection to the external environment by convection [W]; $\dot{\mathbf{Q}}_{\mathbf{Rad}}$ is rate of heat rejection to the external environment by radiation [W]; h is convection heat transfer coefficient [W/m².°C]; T_s is surface temperature analyzed [°C, K for radiation]; T_a is room temperature [°C, K for radiation]; σ is Stefan-Boltzmann constant equal to 5,67 x 10^{-8} [W/m².K^4]; ε is emissivity of the surface analyzed and dA is infinitesimal element of area [m²].

$$\dot{Q}_{Conv} = \int_{\dot{A}rea} h.(T_s - T_{ar})\, dA \quad (3)$$

$$\dot{Q}_{Rad} = \int_{\dot{A}rea} \sigma.\epsilon_{(\lambda,T)}.\left(T_s{}^4 - T_a{}^4\right) dA \quad (4)$$

For the purposes of these equations the unknowns contained therein must be determined. The emissivity value will be determined later in this paper, the surface temperature data will be obtained with thermograms, the room temperature is provided by the dynamometric bench, and the area element can be replaced by the total finned area of the cylinder to determine the heat loss in that region, or even omitted for determination of heat flow per unit of area. It remains then the right convective coefficient value to be determined.

There are a number of considerations concerning the determination of the convection heat transfer coefficient; one is the characterization of flow regime of the fluid surrounding the surface. In natural convection, fluid motion is caused by natural means such as movement caused by difference in fluid density in regions with varying temperature. On the other hand, forced convection happens when an external force, such as a propeller, provokes fluid movement (ÇENGEL, 2002).

ISSN 2176-5480

The convective coefficient varies not only depending on the speed but also on the flow's direction, surface geometry and roughness and viscosity of the fluid. Therefore, establish an analytical solution for the convective coefficient in a finned surface, such as the cylinder of Petter AA1 engine, becomes very complex. Several researchers studied, experimentally, means to determine the convective coefficient for this case.

The work done by Yoshida *et al.* (2006) was specially similar with the situation here presented for considering the condition of stationary engine, which means in their trials were simulated situations where there was no forced cooling fin on the cylinder, only air movement by density difference. Yoshida *et al.* (2006) presented Eq.5 in which h_{mean} is mean convective coefficient [W/m².°C]; u is wind speed [km/h] and p is space between fins [mm].

$$h_{mean} = \left[2{,}47 - \left(\frac{2{,}55}{p^{0{,}4}}\right)\right] u^{0{,}9} + 0{,}0872p + 4{,}31 \tag{5}$$

There is a great similarity between the geometry of the cylinder studied by Yoshida *et al.* (2006) and the cylinder of Petter AA1 engine. Due to this fact, even with an extrapolation in relation to the space between fins, it was decided to use Eq. 5 to determine the average convective coefficient in each test, taking as input data the mean air velocity around the cylinder measured with a MDA-II anemometer and the space between fins of Petter AA1 engine.

Some hypotheses are generally assumed in the study of heat transfer in the engine's cylinders for not being of great impact on the results and decrease the level of complexity. According to Rakopoulos *et al.* (2004), unidimensional treatment of heat transfer by conduction on the cylinder walls is justified since the temperature varies much more rapidly in directions that are perpendicular to the surface. The assumption of constant wall temperature throughout the engine cycle is very reasonable for engines with metal walls of high conductivity, whereas for thermally insulated surfaces with low conductivity materials such as ceramics, surface temperature variations can be critical and this hypothesis should not be assumed.

3. THE INFRARED THERMOGRAPHY

Infrared thermography through cameras is classified as noninvasive technique for temperature measurements as it exempts the direct contact with the mean of interest, unlike thermocouples and thermometers. Thermal radiation is continuously emitted by materials due to molecular and atomic agitation associated with its the internal energy. In thermography, radiation detectors are used to monitor the thermal radiation energy of a surface in the infrared portion of the spectrum and evaluate its temperature.

According to Resende Filho *apud.* Abreu (2009) thermography can also be qualitative and quantitative. The first is based on the evaluation of the thermal exchanges pattern, while the second determines the levels at which the phenomenon occurs. Qualitatively it is possible to identify critical points of heat exchange in a surface and quantitatively evaluate its scale.

The infrared camera is a device that detects infrared radiation and converts it into visible image to the human eye. Besides generating thermograms, it is also possible to obtain temperature data at different points of the generated image. Infrared radiation detected is converted into an electrical signal, the signal is amplified and conditioned by electronic circuits, and then images known as thermograms are generated from this signal.

The reliability of the data obtained by thermographic inspection lies heavily on the position of the camera in relation to the surface of interest. Viewing angle and distance between camera and object should be observed to suit limits of spatial resolution and measurement resolution of the equipment.

As explained by Çengel (2002), heat transfer by radiation between two surfaces depends, among other factors, on the orientation between them. The emissivity is maximum when the viewing angle (θ) is equal to 0°, perpendicular to the surface. The emissivity variation with the angle of view depends on each surface's properties.

The spatial resolution of the imager, also known as Instantaneous Field of View (IFOV) is defined as the projection of a pixel on the analyzed surface. Therefore, the sum of these projections or IFOV equivalent to the equipment field of vision (Field of View - FOV). This parameter is useful to determine the smallest detail of image that can be identified by the camera (SANTOS, 2006).

The maximum distance of an object for it to be detected by the thermal imager can be calculated, as shown by Snell *apud.* Santos (2006), given by Eq. 6 and Eq. 7 in which $X_{máx}$ is maximum distance of an object for it to be detected by the thermal imager [m]; *IFOV* is Instantaneous Field of View [mrad]; *FOV* is Field of View [mrad]; *Pix* is number of pixels from the camera and *X* is smaller dimension for the object [m].

$$IFOV = \frac{FOV}{Pix} \tag{6}$$

$$X_{máx} = \frac{X}{IFOV} = X\frac{Pix}{FOV} \tag{7}$$

ISSN 2176-5480

The measurement resolution is a parameter that relates to the smallest object which can have their temperature measured by the infrared camera at a certain distance. It is also known as Measuring Instantaneous Field of View (MIFOV). According to Snell *apud.* Santos L. D. (2006) measurements performed outside the limit of the measurement resolution are smaller than the actual surface temperature.

According to Santos L. D. (2006) the manufacturers do not declare the value of MIFOV of their equipment, however, this parameter is two to four times smaller than the spatial resolution. Based on this information one can obtain the maximum distance which guarantees an acceptable temperature measurement. Noting that a conservative approach uses the value f equals four.

Equation 8 shows how to calculate the MIFOV, in which XM_{max} is the maximum distance of the object that guarantee precision in temperature measurements [m]; X_{max} is the maximum distance of the object for it to be detected by the infrared camera [m]; f is the reduction factor of measurement resolution relative to spatial resolution.

$$XM_{máx} = \frac{X_{máx}}{f} \tag{8}$$

The biggest uncertainty in thermographic measurements is the emissivity. The emissivity of surfaces is not actually known, therefore it must be estimated. Besides varying with temperature and viewing angle, the emissivity also depends on the surface conditions such as color, rust and dirt. If an error in the emissivity value is assumed, then an error is also committed when the temperature is calculated based on the thermograms. The increase in emissivity can reduce these errors (HOLST, 2000).

The room temperature is also an important input data for setting the emissivity and must be monitored constantly, unless tests last only a few minutes. If the local of test is closed, the conditions remain almost constant (HOLST, 2000).

4. MATERIALS AND METHODS

The research was conducted in the laboratory of the Thermal and Fluid Sciences Department of Federal University of São João del-Rei - UFSJ. A dynamometric bench with hydraulic brake model TD200 Tecquipment - TQ, equipped with data acquisition board and instrumentation that allows the use of VDAS and ECA100 software, torque analysis, power, pressure inside the cylinder, air and fuel consumption, exhaust gases temperature, atmospheric pressure and temperature and engine speed.

Through some adjustments on the bench, the engine model Petter AA1 was installed, single-cylinder, naturally aspirated and air-cooled. The other characteristics of the engine are presented in Table 1. The end result of mounting the Petter AA1 engine on the dynamometric bench is shown in Figure 1.

Table1. Constructive characteristics of Diesel Engine Petter AA11.

Characteristics	Values
Cylinder bore	69,85 mm
Stroke	57,15 mm
Power (3600 rpm)	2,61 kW
Displaced volume	219 cm³
Compression rate	17:1

Font: Petter Manufacturer Manual.

The mixture of 5% by volume of biodiesel in fossil diesel (B S1800), in accordance with ANP resolution No. 42 of 2009, was acquired at regular gas stations. It was chosen to perform the tests in three regimes of operation, namely 1400, 2000 and 3000 revolutions per minute at full load. In the case of tests carried out in this work, the expression "full load" means the position of maximum flow in the injection pump to a condition of full throttle. In relation to the fuel two properties are of great importance in this study for calculating the energy supplied to the engine: density and lower heating value. The values of these properties can vary for different production lots, by the raw materials conditions and process variables. As it was not possible to measure these values for samples of utilized fuel, reference values were searched in the literature. Equation 9 derived by Maziero *et al.* (2007) expresses the behavior of density of diesel fuel according to the fuel temperature, in which ρ is density [kg/m³] and T_{fuel} is fuel temperature [°C].

$$\rho = -0{,}4968 T_{comb} + 867{,}44 \tag{9}$$

ISSN 2176-5480

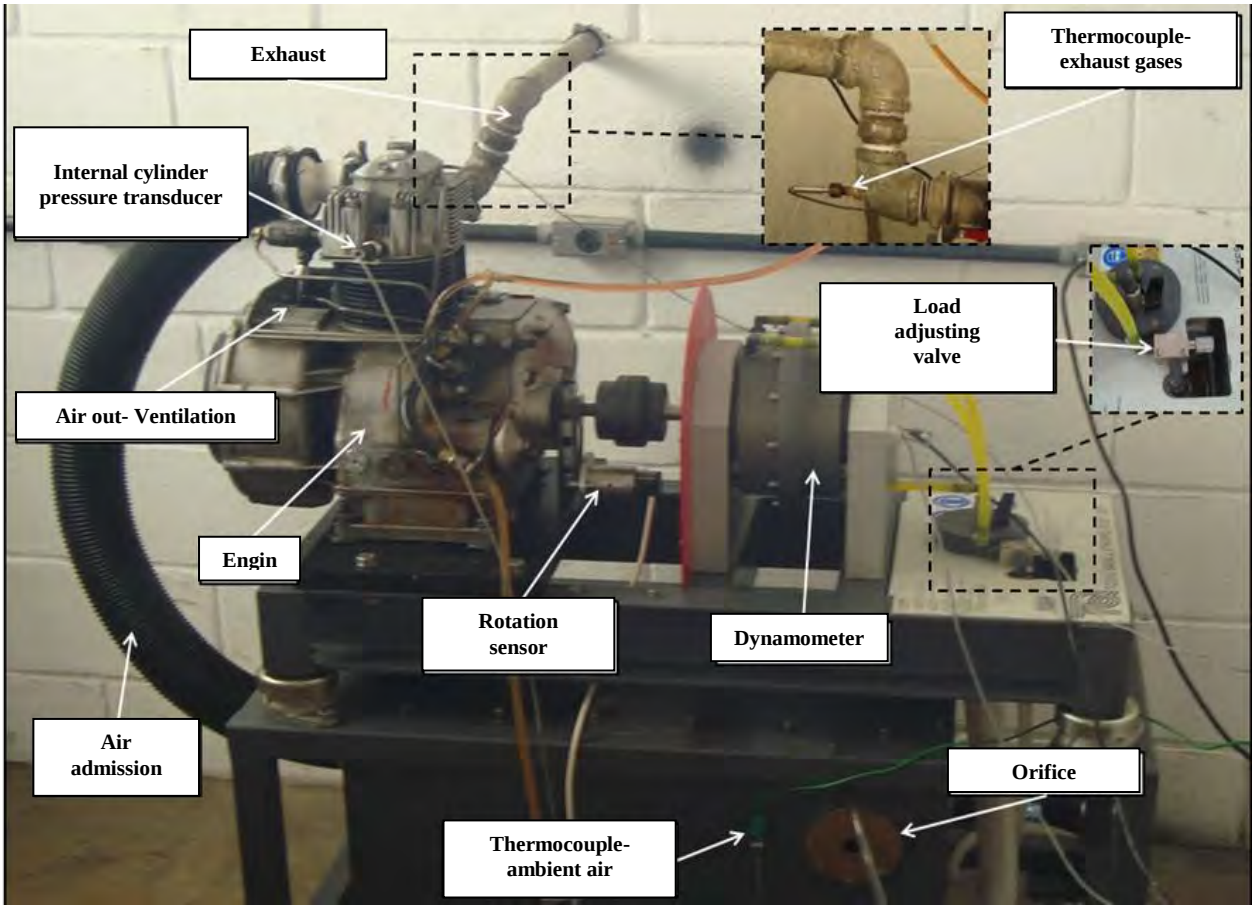

Figure 1. Petter AA1 engine on the dynamometric bench.

The value of lower heating value were taken from Barbosa *et al.* (2008), being 41737.0 kJ / kg for diesel fuel. Each test was repeated three times to confirm the results and between changes in the rotation an interval of 20 minutes was respected. Always before collecting test data, 15 minutes of engine operation and its stabilization were expected, verified through rotation data variation, power, exhaust gas temperature and maximum temperature in the engine cylinder analysis. This latter one was obtained with the infrared camera. Besides the dynamometric bench data, thermograms were recorded simultaneously in each assay, as well as air velocity surrounding the cylinder fins. The air velocity data were collected with a digital anemometer, model MDA-II manufacturer Minipa, this instrument was positioned at half the height of the cylinder.

For thermograms generation the infrared camera FLIR, model T200, was used. The camera is shown in Fig. 2. The characteristics of the imager T200 are shown in Tab. 2.

Figure 2. Infrared camera FLIR T200.
Font: FLIR Manufacturer Manuel

ISSN 2176-5480

Table 2. FLIR T200 thermal imager characteristics.

Characteristics	Type / Values
Temperature range	-20°C to 350°C
Emissivity	Adjust from 0.1 to 1.0
Frame rate	9Hz
Field of Vision (FOV)	25° x 19° (0,436 rad x 0,331 rad)
Minimum Focus Distance	0,4m
Thermal Sensibility (NETD)	<0,8°C a 30°C
Detector type	240 x 180 pixels, focal plane array, uncooled microbolometer
Spectral range	7,5 a 13µm
Measurement correction	Reflected ambient temperature and emissivity correction

Font: FLIR Manufacturer Manual.

As previously reported, it is extremely important to plan the imager position relative to the point of interest, which in this study is the outer surface of the engine cylinder. The position must be the most perpendicular as possible to reduce the error associated with the viewing angle (SANTOS, 2006). The field of view of the thermal imager (FOV) also needs to be considered to ensure that the spatial resolution of the equipment is respected.

As demonstrated above, Equations 6 and 7, the T200 FLIR imager IFOV can be obtained $IFOV_{Horizontal}$ and $IFOV_{Vertical}$ as follows.

$$IFOV_{Horizontal} = \frac{FOV}{Pix} = \frac{0{,}436}{240} \cong 1{,}81 \times 10^{-3} rad$$

$$IFOV_{Vertical} = \frac{FOV}{Pix} = \frac{0{,}331}{180} \cong 1{,}84 \times 10^{-3} rad$$

Taking the maximum engine area of interest as being a square of dimensions 72 mm x 72 mm (0.072 m) corresponding to the height of the finned region of the cylinder, the maximum distance when using this imager, so that its spatial resolution is respected, is obtained as follow. It is important to note that this dimension was only taken as being the smallest dimension of the object for calculating the measurement resolution, the dimension considered to calculate the rejected heat was the real dimension of the external geometry of the cylinder.

$$X_{max} = \frac{X}{IFOV} = \frac{0{,}072}{0{,}00184} = 39{,}13\ m$$

The spatial resolution determines whether the object is detected by the thermal imager, but to be guaranteed the accuracy of temperature measurements the measurement resolution should be observed, that is calculated below for the FLIR T200 thermal imager, again taking as base the dimensions 72 mm x 72 mm, and a reduction factor of 4.

$$XM_{max} = \frac{X_{max}}{f} = \frac{39{,}13}{4} = 9{,}78\ m$$

Seeking the best conditions in the physical arrangement within the laboratory where the tests were conducted it was decided to place the imager 1 meter forward the engine cylinder, in accordance thus with the minimum distance of 0.4 meters indicated by the manufacturer's manual and with distances that guarantee the detection of the object and the accuracy of temperature data.

Considering all these aspects constraints regarding the positioning of the imager relative to the outer surface of the engine cylinder, thermograms were generated within the physical arrangement shown in Figure 3.

The determination of the engine cylinder outer surface emissivity is an important point to ensure accuracy of temperature measured by the thermal imager. One simple but effective technique to determine this value is described by Romiotto Instrumentos de Medição. The technique consists of setting a black tape to the surface, adjust the emissivity to 0.95 and then measure the temperature value of the area covered with adhesive tape. Next, the temperature of an area not covered by the tape but adjacent to it has is measured, most likely the values are different. Finally, the value of emissivity is modified in the thermal imager until the temperature indicated for the area not covered by tape is equal to that of the covered area. In the article published by Abreu *et al.* (2009) on the quantification of heat loss in catenary furnaces through thermography this procedure was successfully applied.

ISSN 2176-5480

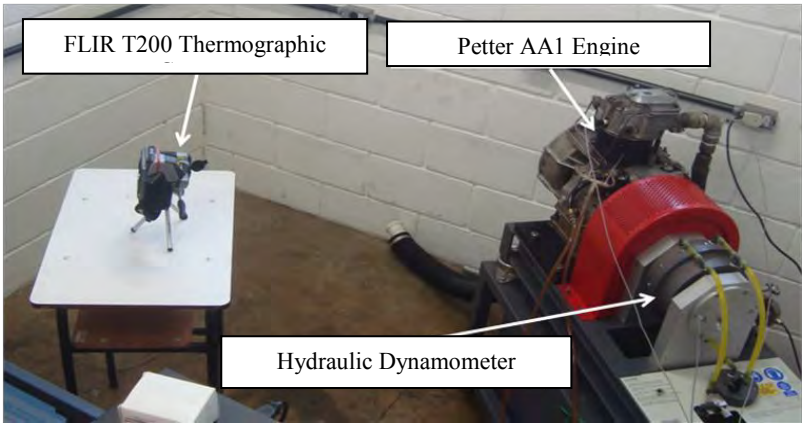

Figure 3. Photograph of the infrared camera position relative to the engine cylinder.

This same technique was used for obtaining the emissivity value of the surface of interest. Using the FLIR QuickReport application version 1.2 provided in conjunction with the infrared camera, it was possible to vary the input value of the emissivity to achieve the desired temperature, in accordance to the procedure previously described. The value obtained then for the emissivity of the analyzed surface was 0.96.

The temperature used to calculate the amount of heat rejected at the finned surface was calculated as the average of all values contained in a matrix of 43 rows and 24 columns, obtained from the central region of each thermogram generated in the essays, as shown in Fig. 4.

This region was chosen for being the one with the lower viewing angle, and for containing all the cylinder vertical length. Values for maximum and minimum temperature in the engine cylinder were also taken from this same matrix, under all conditions tested.

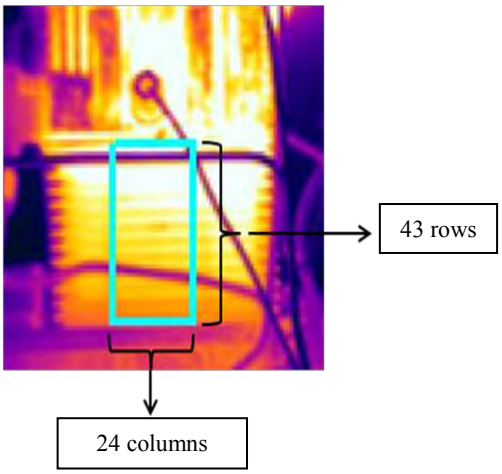

Figure 4. Basis region for temperature matrix generation.

The temperatures matrix of the selected region allows obtaining 1032 values for calculating the average temperature in the cylinder, covering the entire vertical length of the cylinder, along which are noticeable larger temperature variations.

5. RESULTS AND DISCUSSION

Following the methodology previously described on this work, values for the heat rejected through the cylinder finned surface were obtained. Hereafter these values will be presented. The external finned area of the cylinder was calculated from the dimensions shown in Figure 5, considered as approximately 0.183 m². In this calculus the base and top of the cylinder are excluded as they are not exposed to the outside air.

The average convective coefficients of Table 3 were obtained from convective coefficients calculated for each replicate essay at each region of air speed measurement around the fins. The engine has forced ventilation system that had its effectiveness changed due to the withdrawal of the screen that directs air to the fins, therefore making the heat transfer at this region occur by natural convection.

ISSN 2176-5480

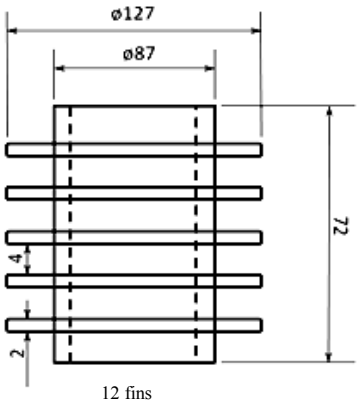

Figure 5. Dimensões do cilindro do motor Petter AA1.

Table 3. Average convection coefficient for engine cylinder finned surface.

RPM	h_{mean} [W/m^2 ^{0}C]
1400	5,12
2000	5,46
3000	6,18

It is intersting to notice that the maximum temperature at the cylinder surface does not vary among the essays. Considering the engine operating at stable regime, due to its own constructive conditions that limitates the thermal exchanges from the cylinder interior to the external surface, the maximung temperature achieved for all engine speed essayed is 150,2ºC. Figure 6 above shows that phenomenon. The green rectangles demarcate the finned region used to collect temperature data and the gray regions are the ones at maximum temperature.

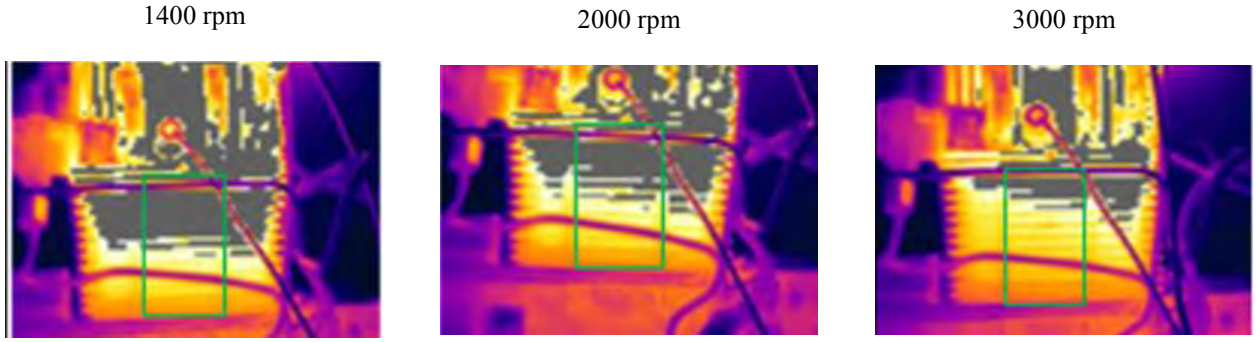

Figure 6. Maximum temperature at the cylinder surface.

According to Table 4, which presents the absolute values of heat loss in the cylinder and the percentage relative to the supplied energy , it appears that this loss decreases with the increase of engine speed. It can be said that the drop in efficiency when the rotation increases, indicates an increase of disability in the combustion process, decreasing the release of energy proportionally. The regime in which the larger absolute heat loss in the cylinder is noticed coincides with the point of greatest efficiency.

Table 4. Energy loss in the cylinder, power and energy supplied to the engine- absolute and percentage values.

	1400 rpm		2000 rpm		3000 rpm	
	[W]	[%]	[W]	[%]	[W]	[%]
Q_0	5533,92	100,00	8231,07	100,00	11940,00	100,00
Potência	577,69	10,44	910,08	11,06	722,69	6,05
Q_{conv}	104,11	1,88	114,20	1,39	119,78	1,00
Q_{rad}	207,59	3,75	214,92	2,61	192,68	1,61
Q_{total}	311,69	5,63	329,11	4,00	312,46	2,61

ISSN 2176-5480

The heat rejected by radiation is almost two times higher than the one rejected by convection. In the case of stationary engine convective coefficient is low and, additionally, the radiation is proportional to the fourth potency of the temperature's differential, where this form of heat exchange becomes more significant.

The reduction in the percentage of energy rejected by the cylinder as rotation increases is due to the fact that, despite increased turbulence in the cylinder favors the thermal exchanges, with the highest velocity of gases, there is less time for these exchanges to occur.

The percentage values for the energy rejected to the environment recorded in this study are consistent with those presented by Ferguson and Kirkpatrick (2001) and Pulkrabek (1997). The first author presents values between 2.6% and 9.2%, and the second author relates variations between 2% and 10%. These authors used the complete energy balance of the engine to calculate how much is rejected to the environment, therefore, did not use direct measures of this portion. Thus, their results consider the entire outer surface of the engine, unlike what has been presented in this work, where the values shown correspond only to the cylinder's finned area. However, it is noteworthy that, out of the outer cylinder area and cylinder head, the substrate's temperature decreases significantly (from 140 º C to 65 º C on average in the case of Petter AA1 engine), decreasing the amount of heat transferred to the environment as well. Therefore it has low impact on the overall heat rejection percentage.

6. CONCLUSION

In this work S1800 B diesel was essayed in a compression ignition engine in order to analyze the amount of heat rejected by the engine cylinder. An infrared camera was used for obtaining thermograms of the region of interest of the study which corresponds to the external finned cylinder area.

Considering only the outer surface of the engine crankcase, therefore excluding the exhaust ducts, the cylinder region is the most critical regarding high temperature. On that surface, the average heat rejected to the atmosphere was of the order of 1700 W / m² for all configurations essayed. For an engine with constructive aspects similar to the Petter AA1 engine, this value can be used for a rapid estimation of quantity of heat rejection relatively to the total external area of the cylinders.

The increase in the rotational speed of the engine causes increased turbulence of load inside the cylinder, a fact that favors the heat exchange through cylinder walls for lifting the convective coefficient. However, with higher speed there is less time for the heat exchange process and this condition has exceeded the contribution of increased turbulence. Therefore, proportionally to the amount of energy supplied to the engine, there was less heat rejection from the cylinder as rotational speed increased, contributing to raising the exhaust gases temperature.

Thermography proved to be a practical and efficient tool, dispensing apparatus mounting on the engine crankcase. With a careful adjustment of emissivity and respecting the distance of the object that ensures the accuracy of measurements, an array of temperatures with large amount of measurement points could be composed. The geometry of the studied area was the greatest limitation found for being cylindrical and made of good electrical conductor material, which limits the field of measurement accuracy by increasing the viewing angle.

7. ACKNOWLEDGEMENTS

The authors express their sincere thanks to the Federal University of São João del-Rei and the CNPq (National Counsel of Technological and Scientific Development) that has funded this research.

8. REFERENCES

Abreu, R. D. A., Brito, J. N., Silva, J. A., Pereira, M. G. and Silva, D. A. 2009. Applied Quantitative Thermography to the Study of Thermal Energy Losses in the External Surface of Ovens Catenary. In: **20th International Congress of Mechanical Engineering**, Gramado, RS.

Alegre, J. A., Velásquez, A. 1993. Simulação dos Processos e Análise Exergética do Motor de Ciclo Diesel. **163 f. Tese (Doutorado) - Universidade Estadual de Campinas**, Campinas, SP.

Barbosa, R. L., Silva, F. M., Salvador, N., Volpato, C. E. S. 2008. Desempenho Comparativo de um Motor de Ciclo Diesel Utilizando Diesel e Misturas de Biodiesel. **Ciência e Agrotecnologia**, v. 32, n. 5, p. 1588-1593, Lavras, MG.

BRASIL. Agência Nacional do Petróleo, Gás Natural e Biocombustíveis (ANP). Resolução nº42, de 16 de dezembro de 2009. Classificação e distribuição do óleo diesel e misturas com biodiesel utilizados no Brasil. **Diário Oficial da União.** Brasília, DF, 17 dez. 2009.

Çengel, Y. A. 2002. Heat Transfer: A Practical Approach. **2 ed. McGraw-Hill**.

Ferguson, C. R., Kirkpatrick, A. T. 2001. Internal Combustion Engines: Applied Thermosciences**.** 2 ed. John Wiley & Sons.

Heywood, J. B. 1988. Internal Combustion Engine Fundamentals. **McGraw-Hill**, New York.

Holst, G. 2000. Common Sense Approach to Thermal Imaging**. The International Society for Optical Engineering,** Washington.

Jóvaj, M. S., Máslov, G. S. 1973. Motores de Automovil. **Editorial MIR**, Moscou.

Maziero, J. V. G., Corrêa, I. M., Úngaro, M. R., Bernardi, J. A., Storino, M. 2007. Desempenho de um Motor Diesel com Óleo Bruto de Girassol. **Revista Brasileira de Agrociência**, v. 13, n. 2, p. 249-255, Pelotas.

Pulkrabek, W. W. 1997. Engineering Fundamentals of the Internal Combustion Engine. 1. ed. Prentice Hall, New Jersey.

Rakopoulos, C. D., Antonopoulos, K. A., Giakoumis, E. G. 2004. Investigation of the temperature oscillations in the cylinder walls of a diesel engine with special reference to the limited cooled case. **International Journal of Energy Research,** v. 28, n. 11, p. 977–1002.

"Romiotto Instrumentos de Medição". 25 set. 2011. <www.romiotto.com.br>

Santos, L. 2006. Termografia Infravermelha em Subestações de Alta Tensão Desabrigadas. **129 f. Dissertação (Mestrado) - Universidade Federal de Itajubá**, Itajubá, MG.

Yoshida, M., Ishihara, S., Murakami, Nakashima, K., Yamamoto, M. 2006. Air-cooling effects of fins on a motorcycle engine. **JSME International Journal,** v. 49, n. 3, p. 869-875, Japan.

9. RESPONSIBILITY NOTICE

The author(s) is (are) the only responsible for the printed material included in this paper.